

Reconstructing With Geometric Moments

Faouzi Ghorbel*, Stéphane Derrode[†], Sami Dhahbi* and Rim Mezhoud*

*Groupe de Recherche Images et Formes de Tunisie (GRIFT),

Laboratoire CRISTAL, Ecole Nationale de Sciences de L'Informatique (ENSI),

Campus Universitaire, 2080 La Manouba, Tunisia

Email: {faouzi.ghorbel, rim.mezhoud}@ensi.rnu.tn

sami.dhahbi@cristal.rnu.tn

[†]EGIM, groupe GSM (CNRS UMR 6133, Institut Fresnel).

Domaine Universitaire de Saint Jérôme, F-13013 Marseille Cedex 20, France,

Telephone: (+33 4 91 28 28 49, Fax: +33 19 1 28 88 13,

Email: stephane.derrode@enspm.u-3mrs.fr

Abstract—It is well-known that an image can be reconstructed from an infinite set of moments. Many works have focused on the reconstruction aspects of orthogonal moments, and have shown that the image can be reconstructed easily from a finite set of orthogonal moments. However, reconstruction ability of geometric moments is not yet proved. In this paper, the inverse problem of geometric moments is addressed. The approach used consists in recovering the Fourier transform of the image from the geometric moments set. Then, the image is reconstructed using the inverse Fourier transform. Both theoretical and experimental results are given.

I. INTRODUCTION

The mathematical concept of moments has been around for many years and has been utilized in many fields ranging from mechanics and statistics to pattern recognition and image understanding. Describing images with moments instead of other more commonly used image features, means that global properties of the image are used rather than local properties. Historically, the first significant work considering moments for pattern recognition was performed by Hu [1]. From methods of algebraic invariants, he derived a set of seven moment invariants, using non-linear combinations of geometric moments. These invariants remain the same under image translation, rotation and scaling. Since then, moments and functions of moments are widely used in pattern recognition [2], ship identification [3], aircraft identification [4], pattern matching [5] and scene matching [6]. In addition, the completeness of their description results in one of their often cited attributes, the ability to reconstruct an object from its set of moments. Unfortunately, the kernel function of geometric moments is not orthogonal, which makes reconstruction of an image from these moments quite difficult [7] and requires moment-matching method [8].

Complex moments was introduced by Abu-Mostafa and Plastis [9] as a simple and straightforward way to derive moment invariants. Like geometric moments, complex moments are not orthogonal. Thus, reconstruction of an image from complex moments is deemed to be quite difficult.

Teague [8] has suggested the notion of orthogonal moments to recover the image from moments based on the theory of continuous orthogonal polynomials, and has introduced both

Zernike and Legendre moments. Other orthogonal moments are Pseudo-Zernike moments [7]. Many works have focused on the reconstruction aspects of orthogonal moments, and have shown that the image can be reconstructed easily from a set of orthogonal moments [7] [8] [10] [11] [12]. Since the continuous orthogonal moments are defined only inside a limit domain ($[-1, 1]$ for Legendre moments, and the unit circle for the case of Zernike and Pseudo-Zernike moments), the computation of those moments require a coordinate transformation. Another problem with the aforementioned moments is the approximation of continuous integrals, which not only leads to numerical errors, but also severely affects the analytical properties which they were intended to satisfy, such as invariance and orthogonality [13].

Recently, to solve this problem, a set of discrete orthogonal moment based on the discrete Tchebichef polynomials are introduced [13]. A second class of discrete orthogonal moments is given by Krawtchouk moments [14] which make use of discrete Krawtchouk polynomials.

Referring back to the basic problem of image reconstruction, it is well-known that an image can be fully reconstructed from the infinite number of its moments. Moreover, the ability to reconstruct a shape from its moment description is often cited as justification for their deployment. Unfortunately, non-orthogonal moments can't define inverse transform. Thus, reconstruction from geometric moments (and other non orthogonal moments such as complex moments) is not straightforward and requires a moment matching technique [8]. However, this method is shown to be impractical as it requires the solution to an increasing number of coupled equations as higher order moments are considered.

In this contribution, the inverse problem of geometric moments is addressed. We show that it is possible to reconstruct the image from its geometric moments. The approach used consists in recovering the Fourier transform of the image from its geometric moments. Then, the inverse Fourier transform is used to recover the image. The symmetry and periodicity properties of Fourier transform are investigated to make this reconstruction possible. Reconstruction results of geometric moments are compared to that of Legendre and Tchebichef

moments.

This paper is organized as follows. In section 2, we recall the definition of geometric, Legendre and Tchebichef moments. Section 3 presents the inverse moment problem, the problems encountered when trying to reconstruct the image with geometric moments, and the solutions proposed in the literature. Section 4 examines how well an image can be reconstructed from geometric moments. Experimental results are given in section 5. A comparison of reconstruction geometric moments ability with Legendre and Tchebichef moments is also provided in this section. Section 6 draws conclusions from this work and presents our future works.

II. MOMENTS

A general definition of moment functions ϕ_{pq} of order $(p+q)$, of an image intensity function $f(x, y)$ can be given as follows:

$$\phi_{pq} = \int_x \int_y \psi_{pq}(x, y) f(x, y) dx dy, \quad (1)$$

where $\psi_{pq}(x, y)$ is the moment weighting kernel. The basis functions may have a range of useful properties that may be passed onto the moments, producing descriptions which can be invariant under rotation, scale and translation. To apply this to digital images, (1) needs to be expressed in discrete form:

$$\phi_{pq} = \sum_x \sum_y \psi_{pq}(x, y) f(x, y). \quad (2)$$

Moreover, the orthogonality property of the basis function is passed onto the moments. Thus, non orthogonal basis functions result in non orthogonal moments, and orthogonal basis functions result in orthogonal moments. Geometric moments are non orthogonal moments, whereas Legendre moments are an example of orthogonal moments.

A. Geometric Moments

Geometric moments are the most popular types of moments and have been frequently used for a number of image processing tasks. The two-dimensional geometric moment of order $(p+q)$ of a function $f(x, y)$ is defined as

$$m_{pq} = \int_{-\infty}^{+\infty} \int_{-\infty}^{+\infty} x^p y^q f(x, y) dx dy. \quad (3)$$

The two-dimensional moment for a $(N \times N)$ discrete image is given by

$$m_{pq} = \sum_{-\infty}^{+\infty} \sum_{-\infty}^{+\infty} x^p y^q f(x, y). \quad (4)$$

Note that the the monomial product $x^p y^q$ is the basis function for this moment definition. Thus, geometric moments are not orthogonal since this basis function is not orthogonal. The uniqueness theorem states that the moment set m_{pq} is unique for a given image function $f(x, y)$. In addition, the existence theorem states that the moments of all orders exist. These two theorems give rise to the reconstruction property of moments.

B. Legendre Moments

The Legendre moments use Legendre polynomials as the basis function. The (p, q) order Legendre moment is defined as:

$$L_{pq} = \frac{(2p+1)(2q+1)}{4} \int_{-1}^1 \int_{-1}^1 P_p(x) P_q(y) f(x, y) dx dy, \quad (5)$$

where the p th order Legendre polynomial is given by:

$$P_p(x) = \frac{1}{2^p p!} \frac{d^p}{dx^p} (x^2 - 1)^p, \quad x \in [-1, 1]. \quad (6)$$

For a given discrete image, the discrete form of Legendre moments is given by:

$$L_{pq} = \sum_{m=0}^{N-1} \sum_{n=0}^{N-1} P_p(m_N) P_q(n_N) f(m, n), \quad (7)$$

where

$$m_N = \frac{2m - N + 1}{N - 1}.$$

Note that the Legendre polynomials are orthogonal over the range $-1 \leq x \leq 1$. Therefore, the image coordinates must be mapped into the limit domain $[-1, 1]$.

C. Tchebichef Moments

Mukandan and al. [13] have suggested the use of discrete orthogonal moments to eliminate the problems associated with continuous orthogonal moments. They introduced Tchebichef moments based on the discrete orthogonal Tchebichef polynomial.

For a given positive integer N (usually the image size), and a value x in the range $[0, N-1]$, the scaled Tchebichef polynomials $t_n(x)$, $n = 0, 1, \dots, N-1$, are defined using the following recurrence relation [13]:

$$t_n(x) = \frac{(2n-1)t_1(x)t_{n-1}(x) - (n-1)(1 - \frac{(n-1)^2}{N^2})t_{n-2}(x)}{n} \quad (8)$$

with the initial conditions

$$\begin{aligned} t_0(x) &= 1, \\ t_1(x) &= (2x + 1 - N)/N. \end{aligned}$$

The Tchebichef moments of order $(p+q)$ of an image $f(x, y)$ are defined as [13]:

$$T_{nm} = \frac{1}{\rho(m, N)\rho(n, N)} \sum_{x=0}^{N-1} \sum_{y=0}^{N-1} t_m(x)t_n(y) f(x, y). \quad (9)$$

where

$$\rho(n, N) = \frac{N(1 - \frac{1}{N^2})(1 - \frac{2^2}{N^2}) \dots (1 - \frac{n^2}{N^2})}{2n + 1}.$$

Since Tchebichef polynomials are orthogonal in the image coordinate space, the computation of Tchebichef moments does not require coordinate transformations.

III. INVERSE MOMENT PROBLEM

To investigate the information content of the higher order moments, the reconstruction power of the moments is analyzed. The inverse problem can be stated as follows : if only a finite set of moments of an image is given, how well can we reconstruct the image?

Consider the Fourier transform for the image function $f(x, y)$:

$$F(u, v) = \int_{-\infty}^{+\infty} \int_{-\infty}^{+\infty} f(x, y) e^{i(ux+vy)} dx dy. \quad (10)$$

Provided that $f(x, y)$ is piecewise continuous and the integration limits are finite, $F(u, v)$ is a continuous function and may be expanded as a power series in u and v , where geometric moments are the expansion coefficient [8] :

$$F(u, v) = \sum_{p=0}^{+\infty} \frac{(-2i\pi)^p}{p!} \sum_{k=0}^p \binom{p}{k} u^{p-k} v^k m_{p-k,k}. \quad (11)$$

From (11) and the two-dimensional inversion formula for Fourier transforms, it follows that

$$\begin{aligned} f(x, y) &= \int_{-\infty}^{+\infty} \int_{-\infty}^{+\infty} F(u, v) e^{-i(ux+vy)} du dv \\ f(x, y) &= \int_{-\infty}^{+\infty} \int_{-\infty}^{+\infty} \sum_{p=0}^{+\infty} \frac{(-2i\pi)^p}{p!} \\ &\times \sum_{k=0}^p \binom{p}{k} u^{p-k} v^k m_{p-k,k} e^{-i(ux+vy)} du dv \quad (12) \end{aligned}$$

However, the order of summation and the integration in (12) cannot be interchanged. Thus we conclude that the power series expansion for $F(u, v)$ cannot be integrated term by term. The difficulty encountered in (12) could have been solved if the basis set $\{u^{p-k}v^k\}$ were orthogonal [12]. Unfortunately, with the Weierstrass approximation theorem [15], the basis set $\{u^{p-k}v^k\}$, while complete, is not orthogonal. Thus, we can deduce that it is not possible to find an inverse transform for geometric moments, which may be used to reconstruct straightforwardly the image from its geometric moments.

To solve this problem, Teague [8] presented two inverse moment transform techniques. The first method, *moment matching*, derives a continuous function

$$g(x, y) = g_{00} + g_{10}x + g_{01}y + g_{20}x^2 + g_{11}xy + g_{02}y^2 + \dots \quad (13)$$

whose moments exactly match the moments, $\{m_{pq}\}$, of $f(x, y)$ through order $Nmax$. However, this method is shown to be impractical as it requires the solution to an increasing number of coupled equations as higher order moments are considered.

The second method for determining an inverse moment transform is based on *orthogonal moments*. Teague observed that the geometric moment definition (3) has the form of the projection onto the non-orthogonal, monomial basis set, $x^p y^q$. Replacing the monomials with a continuous orthogonal basis set results in a continuous orthogonal moment set

with an approximate inverse moment transform. In particular, Legendre moments, which make use of orthogonal Legendre polynomials, are orthogonal moments and have the following inverse moment transform:

$$f(x, y) = \sum_{m=0}^{+\infty} \sum_{n=0}^m L_{m-n,n} P_{m-n}(x_N) P_n(y_N), \quad (14)$$

where

$$x_N = \frac{2x - N + 1}{N - 1}.$$

If only the Legendre moments of order $\leq Nmax$ are given, the function $f(x, y)$ can be approximated by a truncated series:

$$f(x, y) \simeq \sum_{m=0}^{Nmax} \sum_{n=0}^m L_{m-n,n} P_{m-n}(x_N) P_n(y_N). \quad (15)$$

This is actually the basic equation used in image reconstruction via the Legendre moments.

Moreover, discrete orthogonal moments define an exact image reconstruction formula [13] [14]. In particular, the image can be recovered from Tchebichef moments using the following inverse moment transform [13]:

$$f(x, y) = \sum_{m=0}^{N-1} \sum_{n=0}^{N-1} T_{mn} t_m(x) t_n(y). \quad (16)$$

If only the Tchebichef moments of order $\leq Nmax$ are given, the function $f(x, y)$ can be approximated by :

$$f(x, y) \simeq \sum_{m=0}^{Nmax} \sum_{n=0}^m T_{m,n} t_m(x) t_n(y). \quad (17)$$

Thus, unlike continuous and discrete orthogonal moments which define inverse transform, non orthogonal moments can not be used to reconstruct straightforwardly the image since they can not define inverse transform.

IV. RECONSTRUCTION FROM GEOMETRIC MOMENTS

As we have seen in the previous section, it is not easy to find an inverse transform for geometric moments. Nevertheless, we have the relation (11), which may be used to recover the Fourier transform of the image from the set of geometric moments. Thus, we may reconstruct the image from geometric moments since the image can be easily recovered from its Fourier transform.

If geometric moments up to order $Nmax$ are used, then (11) may be approximated by:

$$F_{Nmax}(u, v) = \sum_{p=0}^{Nmax} \frac{(-2i\pi)^p}{p!} \sum_{k=0}^p \binom{p}{k} u^{p-k} v^k m_{p-k,k}. \quad (18)$$

When considering discrete Fourier transform, which is defined as

$$F(u, v) = \sum_{x=0}^{N-1} \sum_{y=0}^{N-1} f(x, y) e^{-2i\pi(\frac{ux+vy}{N})},$$

then (18) becomes:

$$F_{Nmax}(u, v) = \sum_{p=0}^{Nmax} \frac{(-2i\pi)^p}{p!} \sum_{k=0}^p \binom{p}{k} \left(\frac{u}{N}\right)^{p-k} \left(\frac{v}{N}\right)^k m_{p-k,k}. \quad (19)$$

However, the relation (19) cannot be used in practice unless several difficulties are solved. In fact, it is well-known that the higher order moments capture increasingly higher frequencies within a function. To illustrate this remark, we have compared the Fourier transform coefficients computed from the image, to these recovered from geometric moments using relation (19), up to the order $Nmax$. The table (I) gives some Fourier transform coefficients values and the order $Nmax$ needed so that the recovered coefficient $F_{Nmax}(u, v)$ reaches the one computed from the image.

TABLE I
HIGHER ORDER NEEDED SO THAT $F_{Nmax}(u, v)$ REACHES $F(u, v)$.

Coefficient	Value	$Nmax$
$F(0, 0)$	64770	0
$F(0, 1)$	-34100-2521i	19
$F(2, 1)$	7108.8+3355.2i	46
$F(4, 2)$	-573-513.5i	82

We can see in this table that $F_{Nmax}(0, 0)$ reaches $F(0, 0)$ since the first order. In fact, we have $F(0, 0) = m_{00}$. Whereas $F_{Nmax}(0, 1)$, $F_{Nmax}(2, 1)$ and $F_{Nmax}(4, 2)$ reach $F(0, 1)$, $F(2, 1)$ and $F(4, 2)$ only when moments of greater order are used (respectively 19, 46 and 82). Thus, we can deduce that the order needed to recover a Fourier transform coefficient $F(u, v)$ is higher when the sum $(u + v)$ is greater. Another problem encountered when using (19) is that when the sum $(u + v)$ is great, $F_{Nmax}(u, v)$ does not reach $F(u, v)$ even if higher orders are used. Those problems can be solved if we investigate the transform Fourier properties, such as symmetry and periodicity.

We recall that our goal is to decrease the maximum of the sum $(u + v)$ needed to recover the Fourier matrix. Let us divide the Fourier matrix F into four submatrix F_1 , F_2 , F_3 and F_4 , as shown in Fig. (1).

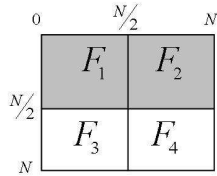


Fig. 1. Fourier matrix divided into four submatrix F_1 , F_2 , F_3 and F_4 .

As a consequence of hermitian symmetry, we have the following relation between Fourier coefficients:

$$F(N - u, N - v) = \overline{F(u, v)}. \quad (20)$$

This relation shows that we have an hermitian symmetry between F_1 and F_4 . Moreover, it is clear that the sum $(u + v)$ of the submatrix F_4 reaches $2N$, whereas it does not exceed N for the case of F_1 . Therefore, as we aim to decrease the maximum of the sum $(u + v)$, we will not compute F_4 using (19) since we can deduce it by hermitian symmetry from F_1 .

In addition, we have the following relation between Fourier coefficients:

$$F(N - u, v) = \overline{F(u, N - v)}. \quad (21)$$

As a result of (21), we have an hermitian symmetry between F_2 and F_3 . Since the sum $(u + v)$ reaches $\frac{3N}{2}$ for both F_2 and F_3 , the use of hermitian symmetry will not decrease in this case its maximum. Nevertheless, it reduces the computational time since recovering a Fourier coefficient using (19) is computationally more expensive than deducing it by hermitian symmetry. We can conclude that we can deduce all the Fourier coefficients if we know only F_1 and F_2 , which are represented by the gray part of the matrix in Fig (1).

We will now investigate the periodicity property of Fourier transform. This property can be expressed by the following relation:

$$F(u, N - v) = F(u, -v). \quad (22)$$

Let F' be the translated matrix of F in v direction by a vector $(-N)$, as shown in Fig. (2). As for the case of F , the matrix F' is also divided into four submatrix F'_1 , F'_2 , F'_3 and F'_4 . From

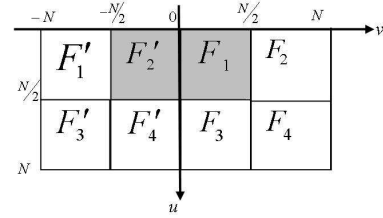


Fig. 2. F and F' represented in coordinates space $(0, u, v)$.

(22), we can conclude that F_2 is equal to F'_2 . Moreover, the sum $(u + v)$ of the submatrix F'_2 does not exceed N , whereas it reaches $\frac{3N}{2}$ for the case of F_2 . That is why we will use (19) to compute F'_2 instead of F_2 . Thus, only F_1 and F'_2 , which represent the gray part of the matrix in Fig. (2), will be recovered using (19). The other submatrix will be deduced from these submatrix using Fourier transform properties.

Thanks to the symmetry and periodicity properties of Fourier transform, the maximum of the sum $(u + v)$ has been decreased from $2N$ to N . The use of those properties has two advantages. On the one hand, the decrease of the maximum of the sum $(u + v)$ is compulsory for image reconstruction. On the other hand, recovering only the half of the Fourier transform result in decreasing by half the computational time.

V. RESULTS

In this section, experimental results are provided to validate the framework developed in the previous section. The binary



Fig. 3. Original letter 'E'.

32×32 letter 'E', shown in Figure (3), is used as the test image.

We have tested the reconstruction from moments using different numbers of moments. The effect of using different thresholds for the reconstructed images was also investigated. In fact, both middle and adaptive threshold [16] are applied to the reconstructed intensity values, to obtain a binary image. The differences between the reconstructed image and the original were measured. The reconstruction error was computed as the total number of pixels that do not have the same value in both the original and the thresholded (reconstructed) binary images. This error is given by the following formula:

$$Erreur = \sum_{x=0}^{N-1} \sum_{y=0}^{N-1} |f(x, y) - T(f_{Nmax}(x, y))|, \quad (23)$$

where $T(.)$ is the middle or adaptive threshold.

Fig.(4), (5) and (6) show the reconstruction results of the binary letter 'E' using respectively an increasing large geometric, Legendre and Tchebichef moments set. The maximum

order of reconstruction, taking values from 10 to 110 in the case of geometric moments and from 6 to 20 for Legendre and Tchebichef moments, are shown in the top of this figure. The basic reconstructions (without threshold) are also given. This figure shows also the thresholded images, the difference images and the reconstruction errors for both middle and adaptive thresholds. The difference images show gray pixels for correct reconstruction, black for pixels incorrectly added, and white for pixels incorrectly removed.

It is clear in Fig. (4), (5) and (6) that increasing the order of moments in reconstruction improves the resulting images. In fact, these three figures show a general improvement in the quality of the basic and thresholded reconstructed images when the order of moments used is increased. In addition, we can see in the differences images that the number of gray pixels (for correct reconstruction) increases, whereas the number of black and white pixels (for incorrectly added or removed pixels) decreases, as the reconstruction order increases. Thus, we can deduce that, like orthogonal moments (Legendre and Tchebichef moments in our study), the quality of the reconstructed image from geometric moments is improved when using higher orders. This remark is confirmed by the plots displayed in Fig. (7). Indeed, Fig. (7) shows the detail plot of the reconstruction error of Geometric, Legendre and Tchebichef moments of the letter 'E', versus the maximum

Order	10	20	30	40	50	60	70	75	80	85	90	95	100	105	110
Basic Reconstruction															
Middle Threshold															
Difference from original															
Error	303	300	245	166	115	33	42	40	48	32	32	32	32	32	32
Adaptive Threshold															
Difference from original															
Error	550	284	238	148	72	16	14	10	10	8	6	6	6	6	6

Fig. 4. Example reconstructions with geometric moments at various orders.

Order	6	7	8	9	10	11	12	13	14	15	16	17	18	19	20
Basic Reconstruction															
Middle Threshold															
Difference from original															
Error	135	111	69	44	29	20	24	9	10	8	6	6	4	3	3
Adaptive Threshold															
Difference from original															
Error	114	112	72	44	26	20	24	10	8	8	6	2	4	2	2

Fig. 5. Example reconstructions with Legendre moments at various orders.

reconstruction order. The reconstruction error is computed up to order 75 for geometric moments, and up to order 20 for Legendre and Tchebichef moments. As can be seen from the Fig. (7), the reconstruction error of various moments decreases as the order of moments used increases.

The second remark is that, for Geometric, Legendre and Tchebichef moments, the adaptive threshold improves better the accuracy of reconstruction compared to middle threshold. It is clear in Fig. (4), (5) and (6) that the number of erroneous pixels is lower when the adaptive threshold is used.

Moreover, we can see in the Fig. (4) that a relatively small finite set of moments may characterize an image adequately. In fact, it is quite clear from this figure that the letter 'E' is recognizable from the reconstruction up to and including order 55. However, it is also clear that the reconstructed image does not match the original. Thus, we can deduce that recognition requires fewer moments than reconstruction.

In addition, compared to orthogonal moments, reconstruction from geometric moments requires higher orders. In fact, if we compare the reconstructed image from geometric moments up to order 75 (Fig. (4)), to the reconstructed images from Legendre moments (Fig. (5)) and Tchebichef moments (Fig. (6)), it is clear that the quality of the reconstructed image from Legendre moments is better even if only Legendre and Tchebichef moments with order lower than 20 are used.

This remark is confirmed by the values of reconstruction error (14 erroneous pixels when reconstructing with geometric moments up to order 70, whereas only 8 erroneous pixels when reconstructing with Legendre and Tchebichef moments up to order 15). In fact, unlike Legendre and Tchebichef moments, geometric moments are not orthogonal, and as a consequence, they suffer from information redundancy. That is why reconstruction from non orthogonal moments (and in particular geometric moments), require higher orders when compared to the reconstruction from orthogonal moments. To test the robustness of Geometric moments in the presence of noise, image 'E' is perturbed with salt and pepper noise. The results are summarized in Fig. (8). It can be seen that higher geometric moments are more sensitive to noise.

Finally, Fig. (9) gives reconstruction results for the binary 32×32 letter 'A'.

VI. CONCLUSIONS

In this paper, the inverse problem of geometric moments has been addressed. We have shown that an image can be reconstructed from a finite set of geometric moments. The proposed method consists in recovering the Fourier transform from the geometric moments, firstly. Then, the image is reconstructed using the inverse Fourier transform. Experimental results showing the reconstructed images and the computed error are given. Both reconstruction error and visual results show

Order	6	7	8	9	10	11	12	13	14	15	16	17	18	19	20
Basic Reconstruction															
Middle Threshold															
Difference from original															
Error	323	304	142	80	49	28	16	8	8	8	7	7	2	3	2
Adaptive Threshold															
Difference from original															
Error	124	114	74	48	26	24	18	10	8	8	6	2	2	2	2

Fig. 6. Example reconstructions with Tchebichef moments at various orders.

that the quality of reconstruction from high order geometric moments is better. When the order goes higher, the difference between the original image and its reconstructed version becomes smaller. Moreover, when compared to continuous orthogonal moments (Legendre moments in our study) and discrete orthogonal moments (Tchebichef moments), geometric moments require higher orders to reconstruct the image. Nevertheless, since geometric moments are computationally less demanding than Legendre and Tchebichef moments, they may be more interesting in real-time applications.

As the image can be reconstructed from geometric moments, we will focus in our future research on the inverse problem of other non orthogonal moments, such as complex moments.

REFERENCES

- [1] M.K Hu, Visual pattern recognition by moment invariants, *IRE Trans. Inf. Theory*, It-8, 1962, 179-187.
- [2] F.L. Alt, Digital pattern recognition by moment invariants, *J. ACM*, 9(2), 1962, 240-258.
- [3] F.W. Smith and M.H. Wright, Automatic ship photo interpretation by the method of moments, *IEEE Trans. Comput.*, 20(9), 1971, 1089-1095.
- [4] S.A. Dudani, K.J. Breeding and R.B. McGhee, Aircraft identification by moment invariants, *IEEE Trans. Comput.*, 26(1), 1977, 39-46.
- [5] H. Dirilten, Pattern matching under affine transformation, *IEEE Trans. Comput.*, 26(3), 1977, 314-317.
- [6] R. Wong and E.L. Hall, Scene matching with invariant moments, *Comput. Vision, Graphics Image Process.*, 8(1), 1978, 16-24.
- [7] C.H. Teh and R.T. Chin, On image analysis by the methods of moment, *IEEE Trans. Pattern Analysis Mach. Intell.*, 10(4), 1988, 496-513.

- [8] M.R. Teague, Image analysis via the general theory of moments, *J. of Opt. Soc. Am.*, 70(8), 1980, 920-930.
- [9] Y. S. Abu-Mostafa and D. Platis, Image normalization by complex moments, *IEEE Trans. Pattern Anal. Mach. Intell.*, PAMI(7), 1985, 46-55.
- [10] J.F. Boyce and W.J. Hossak, Moment invariants for pattern recognition, *Pattern recognition Lett.*, 1(5), 1983, 451-456.
- [11] A. Khotanzad and Y.H. Hong, Invariant image recognition by zernike moments, *IEEE Trans. Pattern Analysis Mach. Intell.*, PAMI(12), 1990, 489-498.
- [12] S.X. Liao and M. Pawlak, On image analysis by moments, *IEEE Trans. Pattern Analysis Mach. Intell.*, 18(3), 1996, 254-266.
- [13] R. Mukandan, S.H. Ong, and P.A. Lee, Image analysis by Tchebichef moments, *IEEE Trans. Image Process.*, 10, 2001, 1357-1364.
- [14] P. T. Yap, R. Paramersan, and S. H. Ong, Image analysis by Krawtchouk moments, *IEEE Trans. Image Process.*, 12, 2003, 1367-1377.
- [15] R. Courant and D. Hilbert, *Methods of Mathematical Physics*, New York: Interscience, 1953, vol. 1.
- [16] S.P. Prismall, M.S. Nixon and J.N. Carter, Accruate object reconstruction by statical moments, *Proceedings of VIE 2003*, 18(3), Guildford, UK, 2003, 1-5.

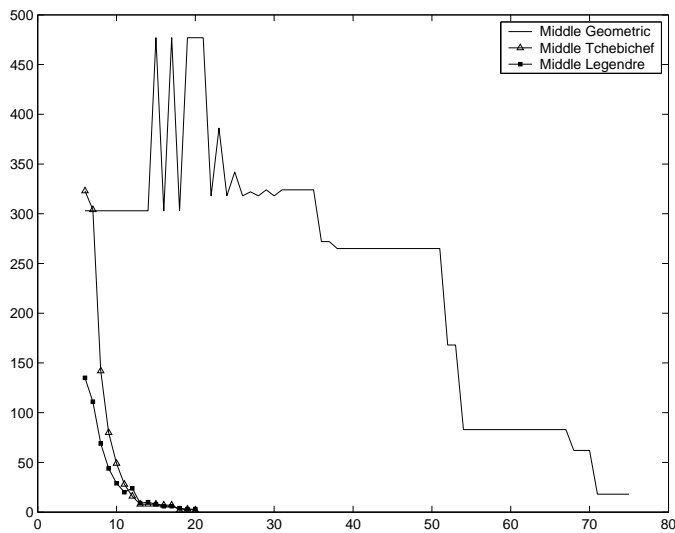


Fig. 7. Reconstruction error of geometric, Legendre and Tchebichef moments of the image 'E' using middle threshold

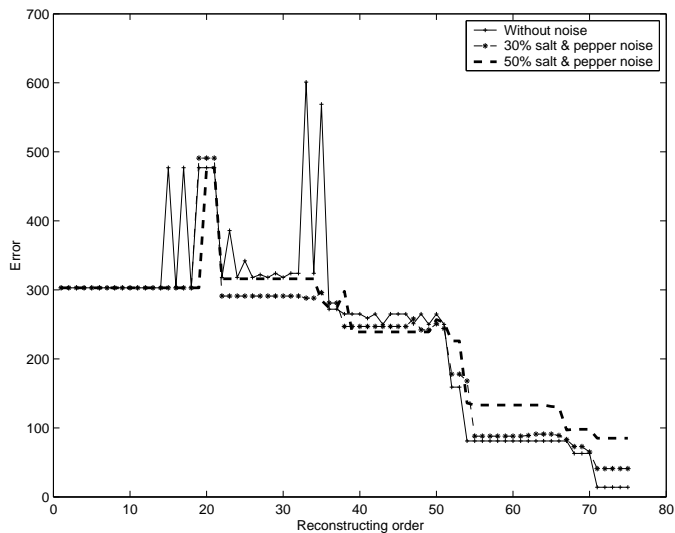


Fig. 8. Reconstruction error of geometric moments of the image 'E' with salt and pepper noise

Order	10	20	30	40	50	60	70	75	80	85	90	95	100	105	110
Basic Reconstruction															
Middle Threshold															
Difference from original															
Error	324	344	143	146	91	67	68	79	79	74	56	56	56	56	56
Adaptive Threshold															
Difference from original															
Error	414	352	144	140	78	38	34	34	34	28	32	32	32	32	32

Fig. 9. Example reconstructions of letter 'A' with Geometric moments at various orders.